AFRL-SR-AR-TR-09-0187

REPORT DOCUMENTATION PAGE

1. REPORT DATE *(DD-MM-YYYY)*	2. REPORT TYPE	3. DATES COVERED *(From - To)*
12-03-2009	Final Report	June 2007-December 2008

4. TITLE AND SUBTITLE
ENVIRONMENTAL EFFECTS ON FATIGUE CRACK GROWTH IN HIGH PERFORMANCE ALUMINUM ALLOYS

5a. CONTRACT NUMBER
FA9550-07-1-0330

5b. GRANT NUMBER

5c. PROGRAM ELEMENT NUMBER

6. AUTHOR(S)
J.J. Williams and N. Chawla

5d. PROJECT NUMBER

5e. TASK NUMBER

5f. WORK UNIT NUMBER

7. PERFORMING ORGANIZATION NAME(S) AND ADDRESS(ES)
School of Materials, Arizona State University, Tempe, AZ 85287

8. PERFORMING ORGANIZATION REPORT NUMBER

9. SPONSORING/MONITORING AGENCY NAME(S) AND ADDRESS(ES)
AFOSR -
875 N Randolph Sr
Arlington, VA 22203
Dr. Joan Fuller/NA

10. SPONSOR/MONITOR'S ACRONYM(S)

11. SPONSOR/MONITOR'S REPORT NUMBER(S)

12. DISTRIBUTION/AVAILABILITY STATEMENT
Distribution A - Approved for Public Release

20090630416

13. SUPPLEMENTARY NOTES

14. ABSTRACT

15. SUBJECT TERMS

16. SECURITY CLASSIFICATION OF:			17. LIMITATION OF ABSTRACT	18. NUMBER OF PAGES	19a. NAME OF RESPONSIBLE PERSON
a. REPORT	b. ABSTRACT	c. THIS PAGE			19b. TELEPHONE NUMBER *(Include area code)*

ENVIRONMENTAL EFFECTS ON FATIGUE CRACK GROWTH IN HIGH PERFORMANCE ALUMINUM ALLOYS

AFOSR Final Report
March 13, 2009

J.J. Williams and N. Chawla
School of Materials
Arizona State University
Tempe, AZ 85287-8706

Background

Aluminum alloys are used in a variety of structural applications, such as aircraft wings, fuselage, etc. In addition to cyclic mechanical loads, these alloys are often subjected to aggressive corrosive environments, e.g., salt water and moisture. Thus, a comprehensive understanding of the combined effects of cyclic mechanical loading and environmental effects is necessary.

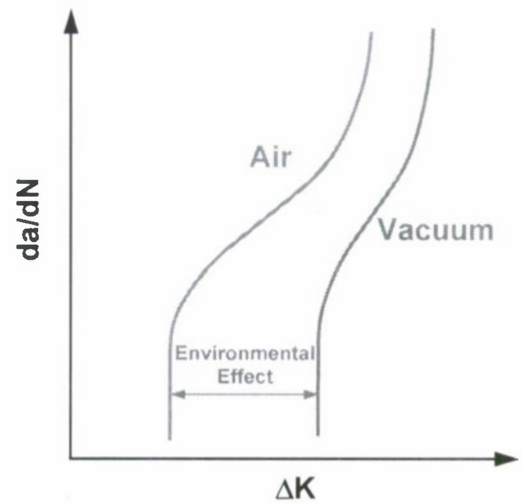

Fig. 1 Schematic of the effect of environment on fatigue crack growth behavior of Al alloys. Testing in air results in a decrease in ΔK_{th}, relative to vacuum.

The fatigue behavior of aluminum alloys is controlled by a variety of factors, such as composition, microstructure, load ratio, and environment [1-10]. In general, it has been found that the fatigue threshold, ΔK_{th}, in vacuum is higher than that in air, Fig. 1. Kirby and Beevers [4], for example, showed that in air, aluminum alloys exhibited decreasing ΔK with increasing R-ratio, while in vacuum ΔK was independent of R-ratio. The differences in fatigue crack growth behavior between air and vacuum environments are not well understood, although a few theories have been proposed [5-10]. These are described in some detail in the next section. Furthermore, the relationship between fatigue crack growth behavior and microstructure evolution during fatigue in vacuum and moisture environments has not really been established. The goal of this AFOSR program was to build a state-of-the-art ultra-high vacuum mechanical testing system, capable of testing in a vacuum environment of 10^{-10} torr, and to investigate the mechanical behavior of 7075 aluminum alloy.

Ultra-High Vacuum Mechanical Testing System

Figure 2 illustrates the vacuum chamber mounted to the MTS 810 load frame. The chamber is isolated from the load train by flexible bellows at the actuator and load cell connections. The

bellows located on the actuator side has a total travel of 100 mm; the bellows on the load cell side has a total travel of 50 mm. The bellows travel allows for actuator displacement, as well as for repositioning the extension rods to accommodate different size samples and grips without having to move the chamber up or down.

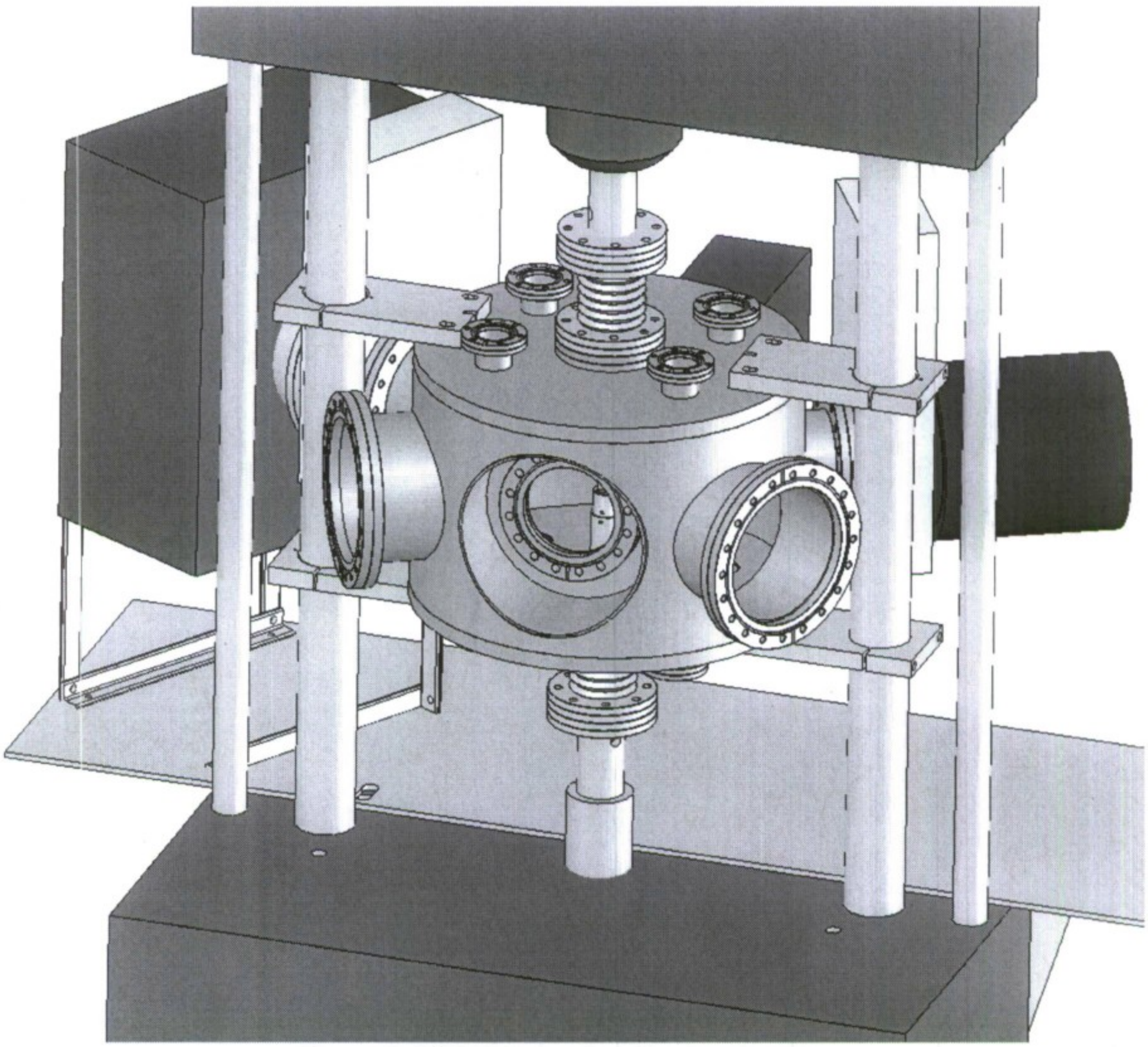

Figure 2. UHV Mechanical Testing System.
• Ion Pump, • **Turbo-Drag pump**, [illegible], • Mass Spectrometer

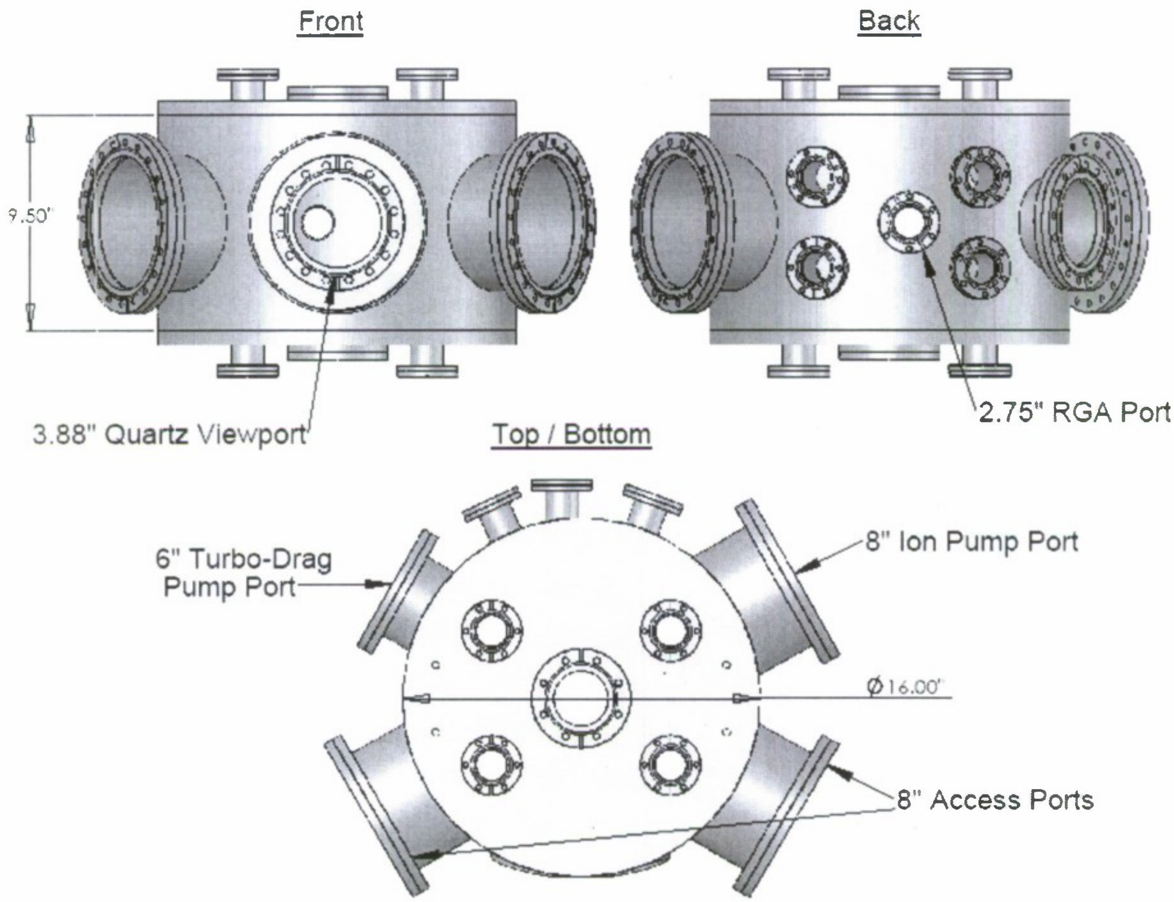

Figure 3. Vacuum Chamber. The twelve unlabelled 2.75" ports are used for vacuum gauges, valves and instrumentation feed-throughs.

The vacuum chamber (Figure 3) is constructed entirely of polished 304L stainless steel, with all welds tested for leaks to a rate of 2×10^{-10} cm^3/s with helium. All devices connected to the chamber, including pumps, gages and valves, are ultra-high-vacuum (UHV) compatible, and all connections are sealed with copper gaskets.

Pumping to $\sim10^{-7}$ torr is accomplished with a 210 L/s trubo-drag pump (Pfeiffer TMU-262P), backed by a 5 L/s scroll pump (ULVAC DIS-250). This pump combination eliminates the possibility of contamination by pumping fluid used in more conventional rotary backed diffusion pump systems. The turbo-drag pump system can be isolated from the chamber by a 6" UHV gate valve. Isolation is necessary when opening the chamber or when using the ion pump. The 300 L/s ion pump (Kurt Lesker LION-300) is used to achieve pressures of $\sim10^{-10}$ torr. Like the turbo-drag pump, the ion pump can be isolated from the chamber by closing an 8" UHV gate valve. As can be seen in Figure 3, both pumps are connected directly to the vacuum chamber to achieve optimum pump-down speeds.

Pumping down the chamber is further facilitated by use of two 500 W quartz lamps located inside the vacuum chamber. At a maximum chamber temperature of 200°C, the lamps efficiently heat up all interior surfaces to remove adsorbed moisture. The lamps, in combination with a programmable controller (Eurotherm 2408) and solid stated relay (Eurotherm TE10A) can also be used for elevated temperature fatigue and thermo-fatigue tests.

Vacuum levels within the chamber are monitored by a thermocouple gauge, nude ion gauge and a quadrupole mass spectrometer. The thermocouple gauge has an operating range of 2 torr to 1×10^{-3} torr. The nude ion gauge has an operating range of 1×10^{-3} torr to 2×10^{-11} torr. The quadrupole mass spectrometer (Hiden Analytical HAL-101) has a partial pressure detection limit of 3.5×10^{-14} torr, a maximum operating pressure of 7×10^{-4} torr and an atomic mass detection range of 1 amu to 100 amu. As illustrated in Figure 4, the head of the mass spectrometer is located 5 mm behind the test specimen. The closeness of the mass spectrometer to the sample will enable rapid detection of changes in atmospheric composition as newly formed surfaces react to the surrounding gases during fatigue crack growth.

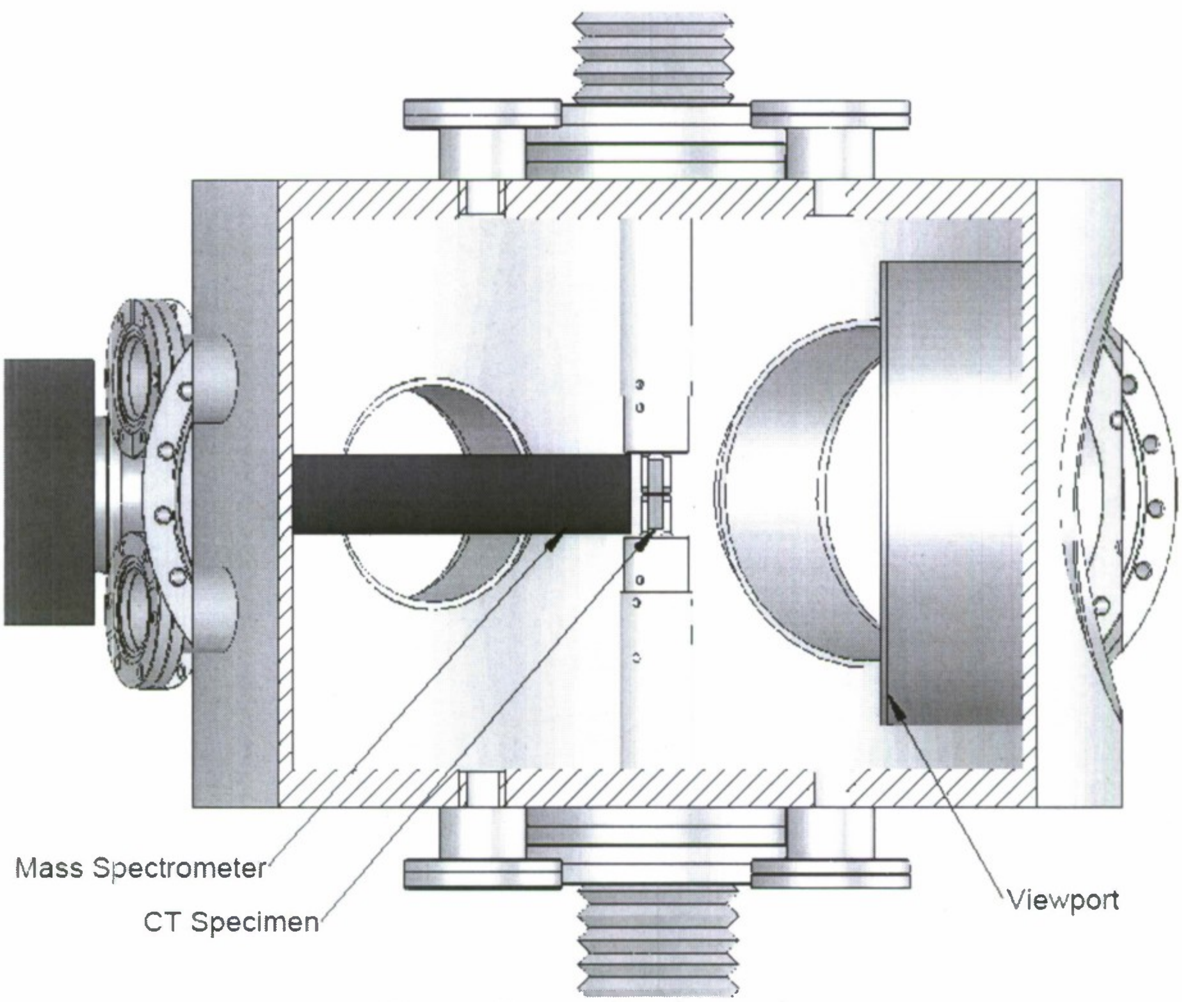

Figure 4. Vacuum Chamber Interior

Also shown in Figure 4 is the recessed viewport, which allows the external microscope (Questar QM-100) to reach its lowest working distance (15 cm) and hence to maximize resolution. The microscope, in combination with a three megapixel CMOS camera (Lumenera Infinity1-3) enables the surface of the CT specimen to be viewed with a resolution of ~0.5 μm/pixel. The inner diameter of the recessed viewport is sufficiently large to allow the microscope to travel 25 mm in any direction about the center of the viewport. The viewport's quartz has a scratch/dig ratio of 20/10, flatness of $\lambda/4$ and one arc minute parallelism. This optical quality ensures negligible distortion of the image by the viewport. In addition to studying crack growth with the optical microscope, a direct current potential drop system (DCPD) can be used to study and dynamically control crack growth rates.

Preliminary fatigue crack growth data on a 7075-T6 aluminum alloy, tested at a vacuum of aroud 10^{-9} torr, at an R-ratio of 0.1 is shown in Figure 5. These results show that the system is fully operational and can generate high quality fatigue crack growth data.

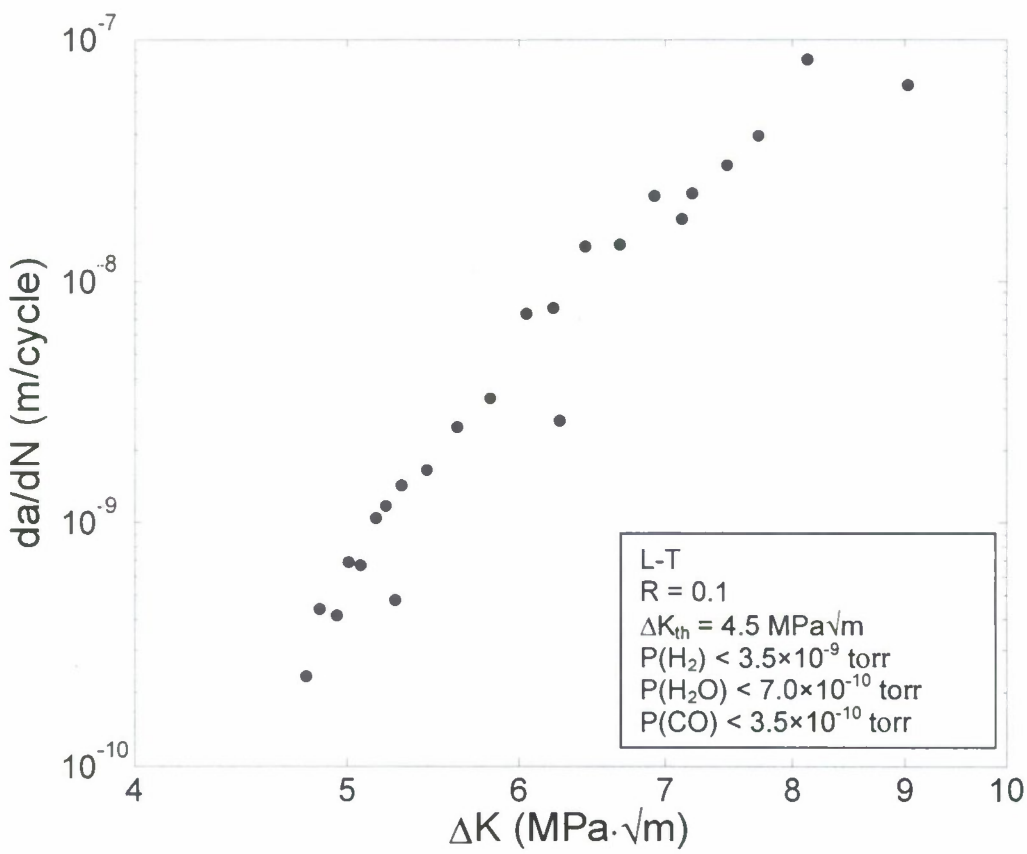

Figure 5. Fatigue crack growth data in 10^{-9} torr vacuum in 7075-T6 Al alloy.